Light Scattering Studies of the *rec*A Protein of *Escherichia coli*: Relationship between Free *rec*A Filaments and the *rec*A·ssDNA Complex†

Scott W. Morrical and Michael M. Cox*

Department of Biochemistry, College of Agricultural and Life Sciences, University of Wisconsin—Madison, Madison, Wisconsin 53706

Received July 25, 1984

ABSTRACT: Light scattering has been used to monitor and distinguish between two types of aggregation reactions observed with the *rec*A protein of *Escherichia coli*. These are (1) the cooperative binding of *rec*A protein to ssDNA in a pathway leading to DNA strand exchange and (2) the formation of free filaments by *rec*A protein in the absence of DNA. Free filament formation requires Mg^{2+}, is very sensitive to ionic strength, and occurs in the absence of single-stranded DNA and RNA. Turbidity measurements indicate that free *rec*A filaments exhibit properties consistent with rigid rods which are 1 μm or more in length. A kinetically distinct nucleation step in free filament formation is observed under some conditions and becomes rate limiting at high pH. Ninety-degree light scattering was employed to measure binding of *rec*A protein to ssDNA under conditions that either favor or block free filament formation. *rec*A protein saturates ssDNA at a stoichiometric ratio of approximately four nucleotide residues per *rec*A monomer. When free filament formation is blocked by various means, the apparent dissociation constant of the *rec*A·ssDNA complex is approximately 10 nM. Under conditions in which free *rec*A filaments form readily, however, the apparent dissociation constant increases to approximately 1 μM. This dramatic decrease in the *observed* affinity of *rec*A protein for ssDNA under conditions that permit free filament formation does not reflect a change in the *intrinsic* affinity of *rec*A protein for ssDNA. Instead, it provides evidence that free filament formation and ssDNA binding by *rec*A protein are competing reactions. Therefore, free *rec*A filaments appear to be structurally and functionally distinct from filamentous complexes of *rec*A protein formed on single-stranded DNA. Free *rec*A protein filaments do not form functional complexes with ssDNA and cannot be considered direct intermediates in *rec*A protein promoted DNA strand exchange reactions.

The *rec*A protein of *Escherichia coli* promotes the exchange of strands between linear duplex and circular single-stranded DNA molecules derived from bacteriophage in vitro. Several phases of this reaction can be distinguished, including the homologous pairing (synapsis) of these species in the presence of ATP or ATPγS,[1] followed by a unidirectional branch migration coupled to the hydrolysis of ATP (Cox & Lehman, 1981a,b). These steps are believed to be analogous to the steps of homologous recombination promoted by the *rec*A protein in vivo. The earliest step in the strand exchange pathway that has been identified to date is the formation of a complex of *rec*A protein on ssDNA (Cox & Lehman, 1982). This step precedes synapsis and has been referred to as a separate phase of the reaction—presynapsis (Radding et al., 1982). In the electron microscope, complexes of *rec*A protein and DNA have been shown to be highly structured filaments that often cover the entire length of DNA molecules thousands of nucleotides long (Flory & Radding, 1982; Di Capua et al., 1982). Several lines of evidence suggest that these structures represent the active form of *rec*A protein. First, stoichiometric, rather than catalytic, quantities of *rec*A protein are required in in vitro strand exchange reactions (Cox & Lehman, 1981a; Cox et al., 1983a; Shibata et al., 1979). Second, there is strong positive cooperativity for ATP binding in DNA-dependent ATP hydrolysis catalyzed by *rec*A protein, although there is believed to be only one nucleotide binding site per *rec*A monomer (Weinstock et al., 1981a,b). Finally, there is a direct correlation between the stability of the *rec*A·ssDNA complexes formed in the first step and the efficiency of the ensuing reaction (Cox et al., 1983a; Soltis & Lehman, 1983).

The SSB protein of *E. coli* enhances strand exchange by increasing the stability of these complexes of *rec*A protein and ssDNA (Cox et al., 1983a). SSB may act, in part, to melt secondary structure in ssDNA (Muniyappa et al., 1984). Evidence has also been presented which suggests a more direct role for SSB in *rec*A·ssDNA complex formation (Griffith et al., 1984). Conversely, ADP destabilizes these complexes, leading to a cessation of branch migration when ADP exceeds 40–60% of the nucleotide pool in a reaction mixture (Cox et al., 1983b). Clearly, the stable interaction of *rec*A protein complexes with ssDNA is of central importance in the mechanism of strand exchange. In order to understand the overall mechanism, we must first understand the nature of the interactions between *rec*A protein and DNA.

Under appropriate conditions (Flory & Radding, 1982; Cotterill & Fersht, 1983), *rec*A protein self-assembles into filaments in the absence of nucleotides, DNA, or SSB. This activity of *rec*A protein is significant in light of the presumed importance of protein–protein interactions in the cooperative binding of DNA and nucleotides and in the mechanical work performed during active strand exchange. These filaments represent an important model system in which monomer interactions can be studied in the absence of DNA. Conceivably, these filaments could be intermediates in the binding of *rec*A protein to ssDNA. Formation of these filaments would then

† This work was supported by National Institutes of Health Grant GM32335. S.W.M. was supported by Training Grant 5-T32 GM07215 from the National Institutes of Health.

[1] Abbreviations: ATPγS, adenosine 5′-*O*-(3-thiotriphosphate); φXss, the circular single-stranded genome of bacteriophage φX174; M13*ori*Css, the circular single-stranded genome of bacteriophage M13*ori*C26; SSB, the single-stranded DNA binding protien of *Escherichia coli*; Tris, tris(hydroxymethyl)aminomethane.

0006-2960/85/0424-0760$01.50/0

be the first step in the pathway leading to *rec*A protein promoted DNA strand exchange. Alternatively, these filaments could represent an unproductive side path in this reaction. To distinguish between these possibilities, it is important to determine whether free *rec*A filaments interact directly with DNA.

One of the most promising approaches to the study of free *rec*A filaments is light scattering (Cotterill & Fersht, 1983). As extremely high molecular weight complexes, *rec*A filaments have a significant turbidity in solution. Filament assembly may thus be directly observed and the filaments characterized based on their light scattering properties (Gaskin et al., 1974). *rec*A·ssDNA complexes are also high molecular weight structures, scattering more light than their individual components due to the second-order dependence of light scattering intensity on radius of gyration. Therefore, light scattering provides a means for observing the physical association of *rec*A protein and ssDNA. This paper describes light scattering experiments that have been performed in an attempt to gain new information on the structure and mechanism of assembly of *rec*A filaments and the *rec*A·ssDNA complex.

Experimental Procedures

*Materials. E. coli rec*A protein was purified as previously described (Cox et al., 1981). The concentration of *rec*A protein in stock solutions was determined by absorbance at 280 nm, using an extinction coefficient of $\epsilon_{280} = 0.59A_{280}$ mg^{-1} mL^{-1} (Craig & Roberts, 1981) and a monomer molecular weight of 37 800. ϕX174(+) circular ssDNA (5.4 kb) was prepared as described (Cox & Lehman, 1981a). M13*ori*C26(+) (Kaguni et al., 1979) circular ssDNA (12 kb) was also prepared by a published procedure. ssDNA concentrations were determined by absorbance at 260 nm, using 36 μg mL^{-1} A_{260} as a conversion factor. All ssDNA concentrations are expressed in nucleotides. *E. coli* exonuclease VII was purchased from Bethesda Research Laboratories; all other biochemicals were purchased from Sigma.

Turbidity Measurements. Apparent turbidities were measured as spectrophotometric absorbance at room temperature in cuvettes of 1-cm path length. Wavelength was varied in the interval 350–590 nm, and *rec*A concentrations were varied from 1 to 4 μM in reaction buffer (5 mM Tris, 5 mM imidazole, 10 mM $MgCl_2$, pH 6.9, 7.5, or 8.1; constant ionic strength maintained with NaCl). Filament formation was initiated by the addition of aliquots of *rec*A protein in storage buffer (20 mM Tris, 1 mM DTT, 0.1 mM EDTA, 10% glycerol, pH 7.5) to reaction buffer. The reported data represent the maximum turbidity observed under each set of conditions. Maximum turbidity was generally achieved after incubation at room temperature for 15–20 min. The data presented in each figure generally were obtained on the same day.

Ninety-Degree Light Scattering. Filament formation kinetics and titration curves for *rec*A·ssDNA complex formation were obtained on an SLM Instruments 8000 series scanning fluorometer, equipped with a thermojacketed cuvette holder attached to a constant-temperature water circulator and with an externally controlled magnetic stirring motor for the sample chamber. This instrument has a focal length of 2 in. (lens to sample), and mean beam path lengths of 128 cm (source to sample) and 105 cm (sample to photomultiplier). Relative light scattering intensities were recorded as fluorometer output at an excitation and emission wavelength of 350 nm and at a constant temperature of 37 °C in all experiments. Cell path length and bandpass were equal to 1 cm and 4 nm, respectively, in all experiments.

Filament Formation Kinetics. Aliquots of *rec*A protein in storage buffer were added to rapidly stirring, temperature-equilibrated cuvettes containing the appropriate reaction buffers (5 mM Tris, 5 mM imidazole, 10 mM $MgCl_2$, pH 6.9–8.1; constant ionic strength maintained with NaCl). For the study of ionic strength effects on filament formation, Tris concentration was varied in 10 mM $MgCl_2$ or NaCl concentration was varied in 10 mM Tris–10 mM $MgCl_2$, all at a constant pH of 7.5. The time courses presented are an average of three experiments.

ssDNA Binding Experiments. Titrations for the formation of the *rec*A·ssDNA complex were carried out in buffers containing 20 mM Tris–1 mM DTT, pH 7.5, or 40 mM Tris–10 mM $MgCl_2$–1 mM DTT, pH 7.5. Small aliquots of *rec*A protein (in 20 mM Tris or 40 mM Tris, pH 7.5) were added successively to temperature-equilibrated cuvettes containing buffer plus ssDNA (generally 3.3 μM ϕXss or M13*ori*Css), and the incremental changes in fluorometer output were recorded. Filament–complex equilibration reactions were carried out in a buffer containing 10 mM Tris–10 mM $MgCl_2$–1 mM DTT, pH 7.5. The reported data reflect the maximum scattering intensity observed in each experiment. All reactions were initiated by the addition of *rec*A protein in storage buffer to solutions of ssDNA in reaction buffer. Reaction mixtures containing variable amounts of ssDNA and *rec*A protein were incubated at 37 °C for 30 min prior to the measurement of relative scattering intensities for each solution.

Nuclease Treatment of recA Stock. Twelve units of *E. coli* exonuclease VII (2 μL of commercial stock solution in 20 mM Tris-HCl, 10 mM 2-mercaptoethanol, 0.05 mM EDTA, and 50% glycerol, pH 8.0) was added to 20 μL of *rec*A protein (4.5 mg/mL in storage buffer), and the mixtures were incubated for 3–4 h at room temperature. Control solutions of *rec*A protein were treated identically, except that exo VII storage buffer, containing no nuclease, was added. The ability of exo VII to remove ssDNA from stock solutions of *rec*A protein was tested by adding sonicated (fragmented) [^{3}H]ϕXss (3.2 $\times$ 10^7 cpm/μmol), final concentration 1.0 μM, to stock *rec*A protein–exo VII mixtures and monitoring the decrease in acid-precipitable counts retained on Whatman GF/C filters with time. Other 20-μL samples of *rec*A stock were treated with 0.9 mg/mL RNase A for 48 h at 4 °C. Filter-binding experiments like those just described tested the ability of RNase A to remove added [^{32}P]RNA (a uniformly labeled 400-bp fragment derived from the SV40 late region, 1.3 $\times$ 10^8 cpm/μmol, a generous gift from David Zarkower of this department) from these solutions.

Results

Polynucleotide Independence of recA Filament Formation. The ability of *rec*A protein to form long filaments in the apparent absence of DNA has been widely reported (Ogawa et al., 1979; McEntee et al., 1981a; Flory & Radding, 1982; Cotterill & Fersht, 1982). The standard purification scheme for *rec*A protein used in this laboratory involves the elution of *rec*A protein from a DNA–cellulose column with 1 mM ATP as the final chromatographic step (Cox et al., 1981). Conceivably, denatured calf thymus DNA could be leached off of this column into the eluate, thus contaminating solutions of *rec*A protein with ssDNA. Subsequent ammonium sulfate precipitation steps should eliminate this contamination; nevertheless, the possibility that the formation of *rec*A filaments is actually a DNA-dependent process supported by ssDNA contamination of *rec*A stock solutions must be considered. A number of observations argue against this possibility. First, added ssDNA does not stimulate the initial rate of *rec*A fi-

lament assembly (S. W. Morrical and M. M. Cox, unpublished results). Second, added ssDNA actually inhibits the final extent of filament formation (see below). Third, A_{280}/A_{260} ratios of *rec*A stock solutions prepared by this method are typically 1.55 or greater. On the basis of the known extinction coefficients of pure *rec*A (Craig & Roberts, 1981) and DNA at 280 and 260 nm, DNA contaminants must comprise 0.06% or less of the UV-absorbing material in *rec*A stock solutions by weight, assuming an ideal A_{280}/A_{260} ratio of 1.6 for pure *rec*A protein.

To further verify the lack of dependence of *rec*A filament formation on DNA, the resistance of *rec*A filament forming activity to nuclease treatment of *rec*A protein stock solutions was tested. *E. coli* exonuclease VII was chosen for these tests because it does not require divalent metal ions, which would interfere with filament formation kinetics by causing *rec*A protein to aggregate in the stock solutions. Exo VII acts processively on 3′ and 5′ ends of single-stranded DNA and therefore should hydrolyze any denatured calf thymus DNA remaining in *rec*A stock solutions. In 4.5 mg/mL *rec*A stock solutions, 500 units/mL exonuclease VII completely converted 1 μM sonicated [^{3}H]ϕXss to acid-soluble material in 3–4 h at room temperature. The same *rec*A stock treated for 4 h with 500 units/mL exo VII formed filaments to the same extent as untreated *rec*A, as observed by 90° light scattering. The initial rate of filament formation was slightly lower than that of the control, possibly due to hydrophobic interactions between *rec*A protein and exonuclease VII. Taken with the observations stated above, these results provide strong evidence that the formation of filaments by *rec*A protein is not dependent upon the presence of small amounts of contaminating ssDNA.

Griffith et al. (1984) observed long filaments of *rec*A protein and RNA formed as a result of RNA contamination of *rec*A stock solutions. The formation of these structures was dependent on the presence of ATPγS, which is not included in our reaction mixtures. Stock solutions of *rec*A protein (4.5 mg/mL) treated with 0.9 mg/mL RNase A for 48 h at 4 °C formed filaments to the same extent as control solutions containing no RNase A. This amount of RNase A completely converted 0.6 μM [^{32}P]RNA added to identical *rec*A solutions to acid-soluble material in the same reaction time under these conditions. As observed in the exonuclease VII experiments described above, the initial rate of filament formation was slightly lower in the presence of RNase A. These results and observations indicate that the formation of free *rec*A protein filaments is not an RNA-dependent process.

Turbidity Studies of recA Filaments. Light scattering by macromolecules small with respect to the wavelength of incident light (including most monomeric protein species at UV and visible wavelengths) is described by the Rayleigh law:

$$I_\theta/I_0 = (B/\lambda^4)(1 + \cos^2\theta)$$

where I_θ/I_0 is the fraction of the incident light intensity scattered to an angle θ and B is a value dependent on the concentration of macromolecules and on their polarizability. To a good approximation, the turbidity of a solution is proportional to the fraction of incident light scattered to all angles by particles in the solution. Therefore, turbidity varies with the inverse fourth power of the wavelength for macromolecules small with respect to the wavelength. Rigid rod-like particles long and narrow with respect to the wavelength exhibit different properties, however. In this case, it has been shown that (1) turbidity varies with the inverse third power of the wavelength, (2) turbidity is directly proportional to the total mass concentration of the scattering particles, and (3) turbidity

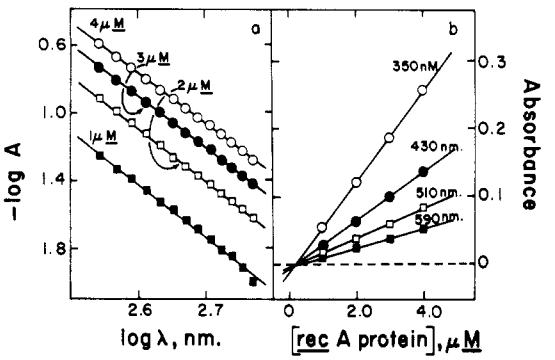

FIGURE 1: Variation of turbidity in aqueous solutions of free *rec*A filaments. (a) Wavelength dependence, λ = 350–590 nm. Solutions contained (○) 4.0, (●) 3.0, (□) 2.0, and (■) 1.0 μM *rec*A monomers in 5 mM Tris, 5 mM imidazole, 10 mM $MgCl_2$, and 2.3 mM NaCl, pH 7.5. (b) Dependence on *rec*A protein concentration at constant wavelength, *rec*A monomer concentration = 1–4 μM; data plotted for representative wavelengths of (○) 350, (●) 430, (□) 510, and (■) 590 nm. All solutions were equilibrated 15–20 min at room temperature prior to data acquisition, to allow maximum polymerization to occur.

is essentially independent of the length distribution of the particles (Gaskin et al., 1974). Under appropriate conditions (to be described below), solutions of *rec*A protein become visibly turbid due to *rec*A protein aggregation. The above three criteria can be applied to determine whether these *rec*A protein aggregates exhibit properties consistent with rigid rod-like structures.

The dependence of turbidity on wavelength for *rec*A aggregates formed at pH 7.5 is shown in Figure 1a. Similar results were obtained at pH 6.9 and 8.1. The average slope of the double logarithmic plots was −3.09 ± 0.06, so that turbidity varied as approximately $\lambda^{-3.1}$. This relationship was independent of *rec*A protein concentration in the interval 1–4 μM. In the same interval, turbidity was linearly dependent on *rec*A protein concentration and therefore on the total mass of filamentous protein in solution (Figure 1b). Results obtained at several different wavelengths were plotted, and the lines intersect at a common point on the horizontal axis, indicating a critical monomer concentration for aggregate formation. This concentration was determined to be 0.22 ± 0.05 μM *rec*A protein, in very close agreement with the value (0.25 μM) previously reported (Cotterill & Fersht, 1983). A critical concentration of approximately 0.2 μM *rec*A protein has been observed previously for other *rec*A activities (Weinstock et al., 1981a). Sonication of *rec*A protein aggregates did not decrease turbidity in any instance. Long sonication times and high power actually caused turbidity to increase, presumably because of solution heating during sonication.

*rec*A protein aggregates satisfy the three requirements of the rigid rod limit (Gaskin et al., 1974), since (1) turbidity varies approximately with λ^{-3}, (2) turbidity is directly proportional to total protein mass, and (3) turbidity is apparently independent of length. This behavior is consistent with the filamentous structure observed by electron microscopy in the absence of DNA, and these structures will be referred to as filaments or free filaments from this point forward. As rigid rods in solution, *rec*A filaments may be quantitatively studied by using simple light scattering measurements, which directly yield the amount of protein present in filaments at a given time. At the same time, light scattering cannot be used as a measure of filament length under conditions in which the rigid rod limit applies. Because rigid rod behavior is observed at wavelengths as high as 590 nm, however, it is reasonable to conclude that *rec*A filaments formed in vitro under the conditions employed

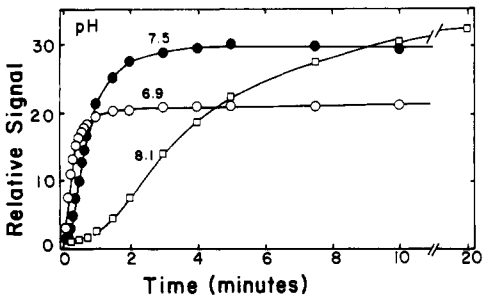

FIGURE 2: Effect of pH on free *rec*A filament assembly. Reactions were carried out at 37 °C in 5 mM Tris, 5 mM imidazole, 10 mM $MgCl_2$, pH 6.9 (○), 7.5 (●), or 8.1 (□). Constant ionic strength was maintained relative to the pH 6.9 mixture by the addition of appropriate amounts of NaCl. The *rec*A monomer concentration was 1.0 μM in all reactions.

in this study have lengths on the order of 1 μm or longer.

pH and Ionic Strength Effects on recA Filament Formation. Both the initial rate and final extent of free *rec*A filament formation varied significantly with pH (Figure 2). The initial rate of filament assembly was highest at pH 6.9, the lowest pH examined in this study, while at pH 8.1, the highest pH tested, a very slow initial rate led to a time lag of approximately 1 min prior to rapid polymerization. This pattern suggests that, at high pH, a kinetically distinct nucleation step becomes the rate-limiting step for filament assembly. The pH dependence suggests that nucleation is dependent on the concentration of the protonated form of at least one amino acid residue. Although the initial rate of filament formation decreases with increasing pH, the total mass of *rec*A protein incorporated into filaments at equilibrium increases with increasing pH. This suggests additional complexity in the ionic interactions involved in this reaction. Filament formation thus appears to be affected by the ionization state of at least one and perhaps several amino acid residues.

As shown in parts a and b of Figure 3, both the initial rate and final extent of *rec*A filament formation are extremely sensitive to moderate increases in the ionic strength of the reaction mixture. The highest total ionic strength used in both figures represents only a 21% increase over control. Increases in either $Tris^+$ or Na^+ ion concentration sharply lower the initial rate of filament formation. The total ionic strengths of the reaction mixtures represented by the curves in Figure 3a are equal to those of the corresponding curves in Figure 3b. Therefore, the $Tris^+$ cation (Figure 3a) has a weaker effect on filament formation than the Na^+ cation (Figure 3b). The final extent of filament formation was optimal at pH 7.5 in 15 mM Tris–10 mM $MgCl_2$. This illustrates again, as in the pH effects described above, that the initial rate and the final extent of *rec*A filament formation are affected somewhat differently by changes in conditions.

ssDNA Binding, Filament Formation Blocked. If *rec*A filaments are intermediates in the interaction of *rec*A protein with single-stranded DNA, then conditions that inhibit filament formation should lower the observed affinity of *rec*A protein for ssDNA. Conversely, if free *rec*A filaments do not interact with ssDNA, then *rec*A filament formation and ssDNA binding reactions should compete, lowering the *observed* affinity of *rec*A protein for ssDNA under conditions that promote filament formation. Therefore, determining the relative affinities of *rec*A protein for ssDNA under conditions that inhibit or promote free filament formation should help to define the relationship between *rec*A filaments and the *rec*A·ssDNA complex.

The formation of *rec*A filaments is prevented when Mg^{2+} ions are deleted from a reaction mixture or, as shown in the last section, when the total ionic strength is raised in the presence of Mg^{2+}. Complexes of *rec*A protein and circular φXss, which scatter much less light than *rec*A filaments at equivalent protein concentrations (see below), can be detected by 90° light scattering when filament formation is blocked by either of these means. Figure 4 shows results obtained from light scattering titrations of φXss with *rec*A protein performed under these conditions. Very similar results were obtained with M13*ori*Css, a circular single-stranded DNA molecule that is over twice the size of φXss. This result confirms that the degree of light scattering we observe is dependent only on the mass of *rec*A protein bound and not on the size of the complexes being formed. To a good approximation, the intrinsic scattering of *rec*A protein varies linearly with *rec*A protein concentration, as shown in control experiments (Figure 4) carried out in the absence of ssDNA. In the presence of ssDNA, the relative degree of light scattering increases sigmoidally with increasing concentration of *rec*A protein and

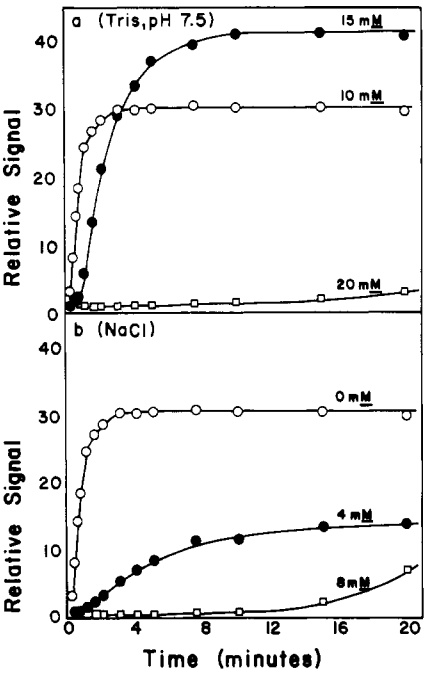

FIGURE 3: Effect of ionic strength on the formation of free *rec*A filaments. (a) Dependence on concentration of Tris buffer: 10 mM (○), 15 mM (●), or 20 mM (□), Tris, pH 7.5, plus 10 mM $MgCl_2$. (b) Dependence on concentration of NaCl: 0 (○), 4 (●), or 8 mM (□) NaCl in 10 mM Tris–10 mM $MgCl_2$, pH 7.5. All reactions were carried out at 37 °C by using 1.0 μM *rec*A monomers. Like symbols in (a) and (b) represent the same total ionic strength: (○) denotes I = 0.076 M, (●) denotes I = 0.084 M, and (□) denotes I = 0.092 M. Data for Figures 2 and 3 were obtained at the same photomultiplier potential and are plotted on the same relative scale.

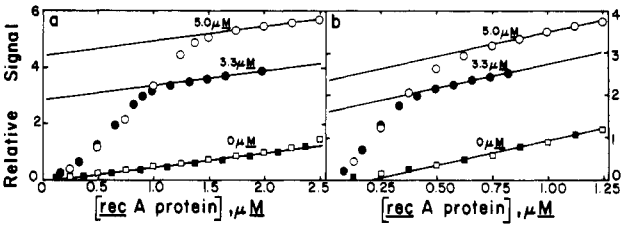

FIGURE 4: Titrations of φX174 ssDNA with *rec*A protein, free filament formation blocked. (a) Reaction in 20 mM Tris–1 mM DTT, pH 7.5. (b) Reaction in 40 mM Tris–10 mM $MgCl_2$–1 mM DTT, pH 7.5. ssDNA concentrations: (○) 5.0 μM; (●) 3.3 μM; (□, ■) 0 μM. The latter two sets of data (□, ■) define the control in both figures: the intrinsic light scattering of *rec*A protein in the absence of ssDNA. Background scattering due to cuvette, buffer, and ssDNA has been subtracted from all data. All titrations were performed at 37 °C.

Table I: Titration Data, Filament Formation Blocked[a]

[Tris] (mM)	[$MgCl_2$] (mM)	[ϕXss] (μM)	stoichiometry[b]	app K_d (nM)[c]	S_{max}[d]	no. of titrations
20	0	3.3	4.0 ± 0.0	8 ± 4		3
20	0	3.3	3.4 ± 0.1	8 ± 1	2900 ± 140	3
20	0	5.0	3.7 ± 0.1	7 ± 4	4460 ± 240	3
40	10	3.3	8.1 ± 0.6	5 ± 1		3
40	10	3.3	9.7 ± 0.3	4 ± 1	1800 ± 60	2
40	10	5.0	10.1 ± 0.1	6 ± 2	2540 ± 10	2

[a] Data obtained from graphs illustrated in Figure 5. All reactions were carried out at 37 °C and at pH 7.5. [b] The calculated ratio of *rec*A protein and ssDNA concentrations at the end point, as estimated from the titration curves. [c] Calculated from titration curves using eq 4, for at least two separate experimental points near the end point of each curve. [d] Vertical intercept of horizontal asymptote in arbitrary units, as plotted in Figure 5.

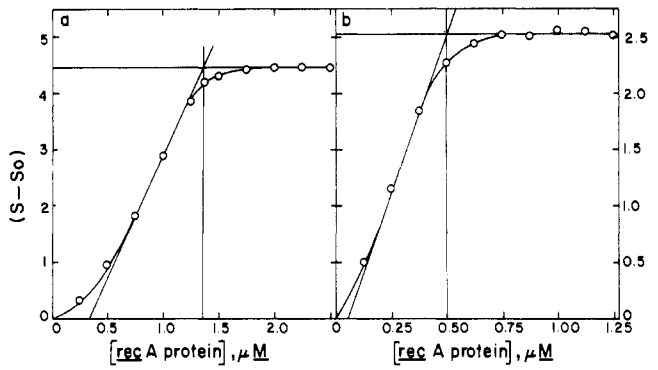

FIGURE 5: Titration curves at 5.0 μM ssDNA, control subtracted. (a) Reaction in 20 mM Tris–1 mM DTT, pH 7.5; corrected data from Figure 4a. (b) Reaction in 40 mM Tris–10 mM $MgCl_2$–1 mM DTT, pH 7.5; corrected data from Figure 4b. Vertical lines mark the titration end points on the horizontal axes. The horizontal asymptotes mark the maximum light scattering intensity for the saturated *rec*A·ssDNA complex. The percent saturation (X value) is determined relative to these values (eq 4) as described in the text.

approaches an asymptote above the inflection point of the curve, indicating that the ϕXss has been saturated with *rec*A protein. The asymptote is in all cases parallel to the line describing the intrinsic scattering due to *rec*A protein. Correcting these data for the intrinsic scattering of free *rec*A protein gives curves with horizontal upper asymptotes (Figure 5), in which vertical coordinates reflect the fractional saturation of ϕXss at a given *rec*A concentration.

The stoichiometric ratios of nucleotide residues bound per *rec*A monomer in the saturated complexes were calculated from the end points of these titrations. The end point of an individual titration curve was defined by the intersection of the horizontal asymptote with the best line drawn through the inflection point. The experiments carried out in 20 mM Tris (typical example shown in Figure 5a) had end points at 3.4–4.0 nucleotide residues per *rec*A monomer. However, in 40 mM Tris–10 mM $MgCl_2$ (typical curve shown in Figure 5b), the stoichiometric ratio generally fell between 8 and 10 nucleotide residues per *rec*A monomer. These data are summarized in Table I. The ϕXss molecule contains significantly more duplex structure at the higher ionic strength (Neuendorf, 1983), which would be relatively inaccessible to *rec*A binding in the absence of the nucleotides ATP or ATPγS (McEntee et al., 1981a). Therefore, the high stoichiometry observed in the latter case (Figure 5b) may reflect a loss of binding sites on ϕXss rather than a change in the binding specificity of the *rec*A protein.

The apparent dissociation constant of the *rec*A·ssDNA complex was estimated from the titration curves in a modification of the procedure used by Silver & Fersht (1983) for fluorescence titrations of etheno-derivatized ssDNA. Assuming that only free *rec*A monomers and monomers bound to ssDNA are present in the reaction mixture (since free *rec*A filament formation is blocked) and ignoring any cooperativity in the binding process, one may express the dissociation constant simply as

$$K_d = [R][SS]/[R{\cdot}SS] \quad (1)$$

where R, SS, and R·SS represent free *rec*A protein, free ssDNA (concentration in *rec*A binding equivalents), and the *rec*A·ssDNA complex, respectively. The concentrations of free *rec*A protein and ssDNA may be expressed as the differences between their total concentrations and the concentration of the *rec*A·ssDNA complex in the solution:

$$[R] = [R]_{tot} - [R{\cdot}SS] \quad (2)$$

$$[SS] = [SS]_{tot} - [R{\cdot}SS] \quad (3)$$

Substitution of eq 2 and 3 into eq 1 yields

$$K_d = ([R]_{tot} - X[SS]_{tot})(1/X - 1) \quad (4)$$

where $X = [R{\cdot}SS]/[SS]_{tot}$ is the fraction of ssDNA bound by *rec*A protein at a given $[R]_{tot}$ and $[SS]_{tot}$. The value of X may be determined (for data near the end points) as the fraction of the maximum height of the titration curve. Apparent K_d values of 5–10 nM were obtained from repeated titrations of ϕXss in 20 mM Tris and in 40 mM Tris–10 mM $MgCl_2$ (Table I). Under both sets of conditions, the formation of free *rec*A filaments is negligible. These results indicate that *rec*A protein binds to ssDNA with relatively high affinity in the absence of free *rec*A filament formation. It should be emphasized that the K_d values obtained in these experiments are apparent dissociation constants only, reflecting the ratio of ssDNA-bound vs. nonbound *rec*A protein at final equilibrium for purposes of comparison. The values reported in Table I were calculated from the high end of the titration curve and reflect only the final 10% of the ssDNA sites occupied by *rec*A protein. The magnitude of K_d may be different at lower protein:ssDNA ratios, though we have not attempted to determine if this is the case. Our calculations treat monomer–ligand binding reactions as independent events and thus do not account for cooperative binding in this system, where the true affinity of *rec*A protein for ssDNA would be a complicated function of the concentrations of free protein, ligand, and preexisting complex.

Implicit in the results described above is the assumption that light scattering intensity is linearly correlated to the amount of *rec*A·ssDNA complex present. Several experiments were conducted to test the validity of this assumption; three observations support the conclusion that light scattering intensity is a valid measurement of the amount of *rec*A·ssDNA complex present in these reaction mixtures. First and most important, the apparent dissociation constants and binding stoichiometries obtained were essentially independent of the ssDNA concentration over the range used in these experiments (Table I). Second, the lower, sigmoidal portions of the titration curves appeared to be identical in experiments performed at different ssDNA concentrations (Figure 4). This indicates that the non-first-order nature of the curves at low *rec*A concentrations is not due to a nonlinear dependence of light scattering in-

tensity on complex size. Instead, the sigmoidal curves obtained are probably the result of cooperative binding at low *rec*A concentrations. Finally, the maximum light scattering intensities attained were directly proportional to the concentrations of ssDNA used in the experiments (Figure 5 and Table I). These observations suggest that light scattering intensity is a quantitative indicator of the amount of *rec*A·ssDNA complex in solution and therefore that the partial saturations of single-stranded DNA derived from titration curves should be accurate.

ssDNA Binding in the Presence of Free recA Filaments. When ssDNA is incubated with *rec*A protein under conditions that favor *rec*A filament formation (i.e., in 10 mM Tris–10 mM $MgCl_2$), the final (equilibrium) scattering intensity is decreased relative to reactions carried out in the absence of ssDNA. The observed decrease in scattering intensity must be caused by the formation of *rec*A·ssDNA complexes, which decreases the total concentration of *rec*A protein involved in free filament formation. While both *rec*A filaments and *rec*A·ssDNA complex contribute to the overall light scattering profile of the solution, we observe a net decrease in scattering intensity since the complexes of *rec*A protein and ϕXss employed in these reactions scatter much less light than *rec*A filaments at equivalent concentrations. In fact, the scattering due to *rec*A·ssDNA complexes was found to be less than the experimental error (~3%) in the measurement of light scattering intensities at all combinations of ssDNA and *rec*A concentrations used in these experiments. Therefore, calculations of the amounts of *rec*A protein sequestered by ssDNA can be made without correcting for scattering by the *rec*A·ssDNA complex, which is effectively zero on this scale.

As described above for free *rec*A filaments, scattering intensity increases linearly with the concentration of *rec*A protein in a control experiment carried out in the absence of ssDNA. In separate experiments, variable amounts of *rec*A protein are incubated with a constant amount of ssDNA and the equilibrium scattering intensities of these solutions are plotted alongside the control (Figure 6). The scattering intensity observed for a given concentration of *rec*A protein is decreased relative to values obtained in the absence of ssDNA, and the deviation is directly proportional to the concentration of ϕXss present. The negative deviation from the control experiment at a given concentration of ssDNA increases with increasing *rec*A protein concentration until an asymptote is reached that is parallel to the control. The approach to this asymptote reflects the saturation of ssDNA with *rec*A protein. Note that a considerable excess of *rec*A protein is required to saturate the ssDNA, compared to the binding experiments carried out in the absence of *rec*A filaments. This implies that the binding of *rec*A protein to ssDNA is much weaker under these conditions.

The horizontal distance between the asymptote and the control curve gives the concentration of protein bound to ssDNA at saturation. This distance was estimated by extrapolating both lines to the horizontal axis. To improve the accuracy and reproducibility of this process, a line was fit to the control data by linear regression. Quadratic equations were fit to the experimental curves by least squares. The asymptotic line was then determined from the slope tangent to the fitted curve at 4 μM *rec*A, the highest protein concentration used. All asymptotic slopes were within 2% of the control slope and were assumed to be equivalent to the control slope. An average stoichiometry of 4.0 ± 0.6 nucleotide residues per *rec*A monomer was obtained, based on data from three separate experiments, each at three different ssDNA concentrations. This

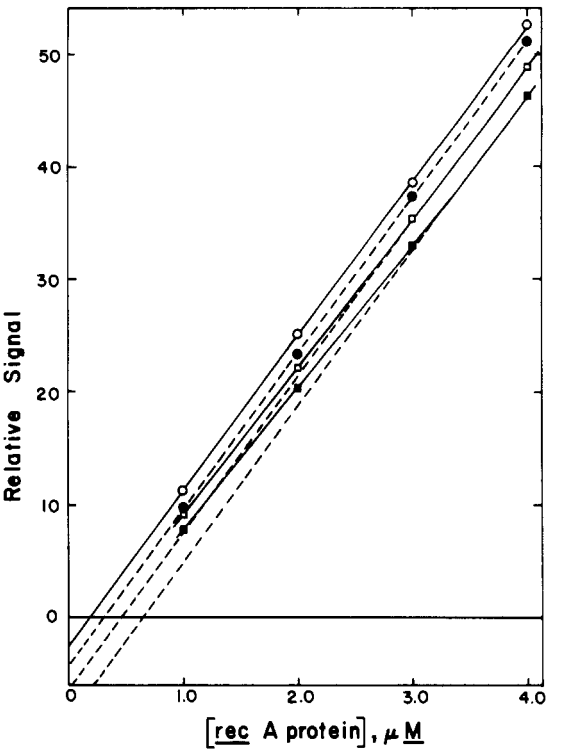

FIGURE 6: Binding of *rec*A protein to ssDNA in the presence of free *rec*A filaments. 1–4 μM *rec*A monomers incubated 30 min at 37 °C in 10 mM Tris–10 mM $MgCl_2$–1 mM DTT, pH 7.5, with (○) 0 μM (control), (●) 0.5 μM, (□) 1.0 μM, and (■) 2.0 μM ϕXss. Control and 0.5 μM ssDNA curves were linear in this range of *rec*A protein concentration and were fit by linear regression. Curves for the 1.0 and 2.0 μM ssDNA data sets were nonlinear and were fit by second-order least squares. Asymptotic slopes for the latter two data sets were defined by the first derivative of the fitted curves evaluated at 4 μM *rec*A protein. All experimental slopes varied from the control by less than 2%, so slopes were set equal to the control slopes and the new asymptotes were "forced" through the experimental point at 4 μM *rec*A protein. For estimation of K_d, the vertical intercept of the control curve was subtracted from all scattering data so that control would pass through the origin.

value is within experimental error of the stoichiometry obtained when filament formation is blocked by the deletion of magnesium.

Since light scattering intensity is directly proportional to filament mass, and since the contribution of the *rec*A·ssDNA complex to light scattering intensity is negligible against a background of highly aggregated *rec*A protein, the fractional saturation of ssDNA can be estimated from the vertical orientation of an experimental point between the control and asymptotes of the curves in Figure 6. Here, the concentration of "free" *rec*A protein (*rec*A in filamentous form, not bound to ssDNA) is given by the expression

$$[R] = Y[R]_{tot} \quad (5)$$

where $Y = s/s_0$ is the ratio of experimental to control scattering intensities at a given *rec*A concentration. It follows that

$$[R{\cdot}SS] = (1 - Y)[R]_{tot} \quad (6)$$

and

$$[SS] = [SS]_{tot} - (1 - Y)[R]_{tot} \quad (7)$$

Substituting eq 5–7 into eq 1 gives K_d in terms of Y:

$$K_d = [[SS]_{tot} - (1 - Y)[R]_{tot}]/(1/Y - 1) \quad (8)$$

The value of Y may be determined from the graph for points at subsaturating levels of *rec*A protein. Equation 8 was used to estimate the apparent dissociation constant of the *rec*A·ssDNA complex under these conditions. An average K_d value

of 0.6 ± 0.2 μM was obtained on the basis of calculations at ten total experimental points in three separate experiments. As for the apparent constants calculated in the last section, this constant cannot be considered to be a true dissocation constant since it ignores the effects of cooperativity. Also, the equations presented in this section assume that the concentration of free *rec*A monomers in solution is negligible.

While interpretation of the constants reported in Table I is subject to limitations already described, the important observation is the large change in the apparent affinity of *rec*A protein for ssDNA under conditions that promote the formation of free *rec*A filaments, rather than the absolute magnitude of these constants. The apparent K_d determined here for the *rec*A·ssDNA complex formed in the presence of *rec*A filaments is approximately 100-fold greater than the observed dissociation constant of this complex under conditions in which *rec*A filament formation is blocked. This decrease in the apparent affinity of *rec*A protein for ssDNA is not due to competition from Mg^{2+} ions, since the experiments discussed in the previous section demonstrated that the apparent K_d of *rec*A·ssDNA is independent of Mg^{2+}. The lower observed affinity is most easily explained if *rec*A filament formation and *rec*A·ssDNA complex formation are competing reactions. Then filament formation would shift the *rec*A·ssDNA dissociation equilibrium to the right, making it more difficult to saturate ssDNA at low *rec*A protein concentrations.

The rate of transfer of *rec*A protein from free filaments to ssDNA can be measured by adding ssDNA to preformed *rec*A filaments and monitoring the decrease in net light scattering intensity with time. The initial rate of transfer increases as the concentration of ssDNA is increased. The half-time for the approach to equilibrium is approximately 1 min. The time course for transfer resembles a multiphase exponential decay (S. W. Morrical and M. M. Cox, unpublished results), so either dissociation of *rec*A protein from free filaments is not a simple first-order process or the dissociation step is not strictly rate limiting throughout the time course for transfer.

Discussion

Our principal conclusion is that formation of free *rec*A protein filaments is a reaction that competes with the binding of *rec*A protein to ssDNA. This conclusion supports the suggestion of Cotterill & Fersht (1983) that the DNA-independent formation of filaments is not on the normal reaction pathway for *rec*A protein promoted DNA strand exchange. It also implies that *rec*A filaments formed in the absence of DNA do not bind to ssDNA in their intact form. Instead, *rec*A protein must be exchanged between free filaments and *rec*A·ssDNA complexes via a dissociative mechanism with a smaller unit (perhaps a monomer or dimer) as an intermediate. This conclusion in no way alters the previous perception that the active species in *rec*A protein promoted reactions is a highly structured complex involving stoichiometric amounts of *rec*A protein bound to DNA. These results may imply that the structures formed in the presence and absence of DNA are functionally and to some extent structurally distinct. Alternatively, the structure of filaments could be very similar to the structure of *rec*A·ssDNA complexes as suggested by recent studies employing electron microscopy. In this case, it must be assumed that binding of intact free *rec*A filaments to ssDNA is precluded by steric considerations. Substantial evidence has accumulated that documents the importance of protein–protein interactions in all types of *rec*A protein promoted reactions. Preformed *rec*A filaments do not appear to bind DNA, however; therefore, free filament formation cannot precede DNA binding in the normal reaction pathway leading

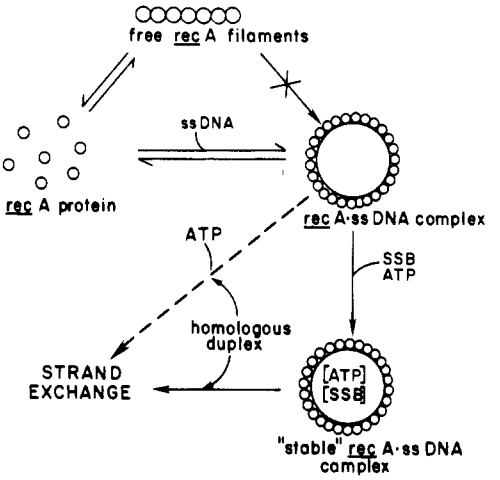

FIGURE 7: Relationship of free *rec*A filaments to *rec*A protein promoted DNA strand exchange.

to DNA strand exchange. The formation of functional *rec*A protein complexes on ssDNA must involve the cumulative addition of small intermediates. The relationship between *rec*A filaments and the strand exchange pathway is diagramed in Figure 7.

In the absence of DNA, *rec*A protein rapidly forms filaments in 10 mM $MgCl_2$ and moderate concentrations of Tris buffer at pH 7.5. The observation that these filaments exhibit the light scattering properties of rigid rods in solution has important implications for the structure and mechanism of assembly of filaments and for the use of filaments as a model system for studying interactions between *rec*A monomers. To the extent that free *rec*A protein filaments exhibit the characteristics of rigid rods in our experiments, some inflexibility on the part of filaments is implied. This suggests that a higher order structure stabilizes a linear filament along its long axis. Electron micrographic studies (Flory & Radding, 1982) indicated a maximum filament width of 16 nm, which would accommodate two to three *rec*A monomers on the basis of the molecular weight of *rec*A protein and by assuming a globular monomeric structure. *rec*A protein crystallizes in continuous helical arrays with one monomer as the asymmetric unit (McKay et al., 1980). In light of these findings, our results are consistent with a helical structure or an oligomer-based structural unit for *rec*A filaments, as opposed to the simple linear structure depicted in Figure 7. Our data indicate that *rec*A filaments are very long under the conditions employed in our turbidity studies, with lengths on the order of 1 μm or greater. Flory & Radding (1982) found filament lengths on the order of 100 nm, but their reactions were carried out at ionic strengths that we have found to be inhibitory to filament assembly. Therefore, our length estimates do not seem unreasonable.

Light scattering provides a means for directly measuring the binding of *rec*A protein to ssDNA and for estimating apparent stoichiometries and relative affinities in the *rec*A·ssDNA complex. We have observed an approximate 4:1 stoichiometry of ssDNA to *rec*A protein at relatively low ionic strengths in the presence and absence of *rec*A filament formation. This suggests that *rec*A binds to a tetranucleotide unit on ssDNA, when it is assumed that all *rec*A protein in the complex is bound directly to ssDNA and not attached in multiple layers via protein–protein interactions. Previous estimates of the stoichiometry of *rec*A·ssDNA complexes have generally ranged from three to six nucleotide residues per *rec*A monomer (McEntee et al., 1981b; Silver & Fersht, 1982; Dombroski et al., 1983). A value of six bases per monomer

was obtained from fluorescence titrations of etheno-derivatized ssDNA (Silver & Fersht, 1982). We prefer our lower value of four bases per monomer, since our measurements were conducted by using a natural ligand (*rec*A exhibits enhanced affinity for modified nucleotide residues in etheno-ssDNA). The low apparent dissociation constant we observed for the *rec*A·ssDNA complex when filament formation was blocked indicates that *rec*A protein has a higher affinity for ssDNA than has previously been observed. It is consistent with the observation that *rec*A·ssDNA complexes are stable, dissociating with a half-time of greater than 30 min, as deduced from nuclease protection experiments (Bryant et al., 1984). Our results show that, depending on reaction conditions, failure to take the aggregation state of non-ssDNA-bound *rec*A protein into account can lead to as much as a 100-fold overestimation of this constant. This is a direct result of the inability of *rec*A filaments and ssDNA to interact directly.

Experiments have been reported that indicate that *rec*A protein dissociates rapidly from ssDNA (Cox et al., 1983a). In these experiments, subsaturating amounts of *rec*A protein were preincubated with ssDNA. A second population of ssDNA was then added, followed by ATP and SSB (to prevent further dissociation) and finally by duplex DNA. The extent of strand exchange observed subsequently for each population of ssDNA with added duplex DNA reflected the amount of *rec*A protein on the ssDNA at the time of addition of the ATP and SSB. These experiments indicated that *rec*A protein equilibrates between two populations of ssDNA with a half-time of 17 s. These results would appear to conflict with the more recent studies of Bryant et al. (1984) mentioned above. The present study suggests a way to reconcile these results. The earlier conclusion was, in part, based on the assumption that all of the *rec*A protein in the preincubation mixture was bound to the first population of ssDNA. This assumption was almost certainly in error, given the conditions under which the preincubations were carried out (25 mM Tris, 10 mM $MgCl_2$). Our present study would indicate that much of the *rec*A protein in the preincubation mixtures was organized in free *rec*A protein filaments and not bound to ssDNA as originally assumed. The rapid binding of *rec*A to challenge ssDNA reflected the binding of free *rec*A protein rather than protein that had dissociated from other ssDNA molecules.

This reinterpretation of results involving ssDNA binding by *rec*A protein does not affect the conclusion that SSB stabilizes these complexes in the presence of ATP. ATP accelerates the dissociation of *rec*A protein from ssDNA 20–30-fold (McEntee et al., 1981a; Bryant et al., 1984). SSB inhibits this dissociation (Cox et al., 1983a), a conclusion that is fully supported by recent observations employing light scattering (S. W. Morrical and M. M. Cox, unpublished results). ATP is required for the formation of stable complexes of *rec*A protein and ssDNA in the presence of SSB (Cox & Lehman, 1982).

We would add one additional note. The DNA-independent formation of *rec*A filaments exhibits a strong sensitivity to ionic strength. This reaction declines precipitously between 20 and 35 mM Tris, a range of buffer concentrations that have been employed routinely by many research groups in the study of *rec*A protein. This very remarkable effect of buffer concentration on a reaction that competes with binding to ssDNA suggests that extreme caution should be observed when comparing results obtained at different buffer concentrations.

References

Bryant, F. R., Taylor, A. R., & Lehman, I. R. (1984) *J. Biol. Chem.* (in press).

Cotterill, S. M., & Fersht, A. R. (1983) *Biochemistry 22*, 3525–3531.

Cox, M. M., & Lehman, I. R. (1981a) *Proc. Natl. Acad. Sci. U.S.A. 78*, 3433–3437.

Cox, M. M., & Lehman, I. R. (1981b) *Proc. Natl. Acad. Sci. U.S.A. 78*, 6018–6022.

Cox, M. M., & Lehman, I. R. (1982) *J. Biol. Chem. 257*, 8523–8532.

Cox, M. M., McEntee, K., & Lehman, I. R. (1981) *J. Biol. Chem. 256*, 4676–4678.

Cox, M. M., Soltis, D. A., Livneh, Z., & Lehman, I. R. (1983a) *J. Biol. Chem. 258*, 2577–2585.

Cox, M. M., Soltis, D. A., Lehman, I. R., DeBrosse, C., & Benkovic, S. J. (1983b) *J. Biol. Chem. 258*, 2586–2592.

Craig, N. L., & Roberts, J. W. (1981) *J. Biol. Chem. 256*, 8039–8044.

DiCapua, E., Engel, A., Stasiak, A., & Koller, T. (1982) *J. Mol. Biol. 157*, 87–103.

Dombroski, D. F., Scraba, D. G., Bradley, R. D., & Morgan, D. A. (1983) *Nucleic Acids Res. 11*, 7487–7504.

Flory, J., & Radding, C. M. (1982) *Cell (Cambridge, Mass.) 28*, 747–756.

Gaskin, F., Cantor, C. R., & Shelanski, M. L. (1974) *J. Mol. Biol. 89*, 737–758.

Griffith, J., Chrysogelos, S., Register, J., & Welsh, G. (1984) *Cold Spring Harbor Symp. Quant. Biol.* (in press).

Kaguni, J., LaVerne, L. S., & Ray, D. S. (1979) *Proc. Natl. Acad. Sci. U.S.A. 76*, 6250–6254.

McEntee, K., Weinstock, G. M., & Lehman, I. R. (1981a) *J. Biol. Chem. 256*, 8835–8844.

McEntee, K., Weinstock, G. M., & Lehman, I. R. (1981b) *Prog. Nucleic Acid Res. Mol. Biol. 26*, 265–281.

McKay, D. B., Steitz, T. A., West, S. C., & Howard-Flanders, P. (1980) *J. Biol. Chem. 255*, 6662.

Muniyappa, K., Shaner, S. L., Tsang, S. S., & Radding, C. M. (1984) *Proc. Natl. Acad. Sci. U.S.A. 81*, 2757–2761.

Neuendorf, S. K. (1983) Ph.D. Thesis, University of Wisconsin—Madison, Madison, WI.

Ogawa, T., Wabiko, H., Tsurimoto, T., Horii, T., & Masukata, H. (1979) *Cold Spring Harbor Symp. Quant, Biol. 43*, 909–915.

Radding, C. M., Flory, J., Kahn, W. R., DasGupta, C., Gonda, D., Bianchi, M., & Tsang, S. S. (1982) *Cold Spring Harbor Symp. Quant. Biol. 46*, 821–828.

Shibata, T., Cunningham, R. P., DasGupta, C., & Radding, C. M. (1979) *Proc. Natl. Acad. Sci. U.S.A. 76*, 5100–5104.

Silver, M. S., & Fersht, A. R. (1982) *Biochemistry 21*, 6066–6072.

Silver, M. S., & Fersht, A. R. (1983) *Biochemistry 22*, 2860–2866.

Soltis, D. A., & Lehman, I. R. (1983) *J. Biol. Chem. 258*, 6073–6077.

Weinstock, G. M., McEntee, K., & Lehman, I. R. (1981a) *J. Biol. Chem. 256*, 8829–8834.

Weinstock, G. M., McEntee, K., & Lehman, I. R. (1981b) *J. Biol. Chem. 256*, 8845–8849.